Physica E 64 (2014) 39–44

Contents lists available at ScienceDirect

Physica E

journal homepage: www.elsevier.com/locate/physe

Thermoelectric transport properties of a T-coupled quantum dot: Atomic approach for the finite U case

E. Ramos [a], R. Franco [a,*], J. Silva-Valencia [a], M.S. Figueira [b]

[a] Departamento de Física, Universidad Nacional de Colombia, A. A. 5997 Bogotá, Colombia
[b] Instituto de Física, Universidade Federal Fluminense (UFF). Avenida litorânea s/n, CEP: 24210-346 Niterói, Rio de Janeiro, Brazil

ARTICLE INFO

Article history:
Received 24 March 2014
Accepted 25 June 2014
Available online 5 July 2014

Keywords:
Quantum dot
Kondo effect
Transport
U finite atomic approach
Thermoelectric effect
Thermomagnetic effect

ABSTRACT

We study thermoelectric transport properties through a gate defined T-coupled quantum dot, describing the system at base with the single impurity Anderson model (SIAM), whose corresponding Green's functions are calculated employing the finite correlation U atomic approach. We compute, with the linear approximation for the thermoelectric transport coefficients, the electrical and thermal conductance (G and K), the thermopower S, the product of the thermoelectric figure of merit and the temperature ZT, for all the regimes of the SIAM: empty quantum dot, intermediate valence, Kondo, and double occupation, at different temperatures; the treatment employed extends the results obtained for the limit of infinite U-Coulomb repulsion in the quantum dot, and has a many-body character, which is absent in Green's function descriptions that employ mean field approximations. Our main result connects the ZT behavior with the interplay between the thermopower and the violation of the Wiedemann–Franz relation; the results are in good agreement with other recent theoretical papers that employ the numerical renormalization group (NRG), different Green's function approximations, and some experimental reports.

1. Introduction

The possibility of employing nanoscopic systems as thermal rectifiers, that enhance efficiency of the macroscopic devices through control of the energy transport on a microscopic scale, is responsible for the renewed interest in the thermoelectric effects of nanoscopic systems in the last few years [1–15]. The necessity of reducing the de-coherent effects linked with the temperature, in order to obtain and control the entanglement states for the quantum computation, is a strong motivation for researching the physics linked to the refrigeration process in nanoscopic systems.

Recently, the experimental realization of nanoscopic thermal rectifiers was reported [8], as well as Coulomb control over the refrigeration process in a mesoscopic system [12]. In this paper, we study the electrical conductance (G), thermopower (S), thermal conductance (κ) and the product of the thermoelectric figure of merit and the temperature (ZT), in a single quantum dot (QD) side coupled to a quantum wire modeled by a ballistic channel, as a function of the gate voltage, which controls the energy level of the QD.

To solve the problem we employed the finite correlation U version of the Atomic Approach (UAP) treatment for the single Anderson impurity model (SIAM) [16]. This treatment presents a many-body character that originates the Kondo effect, in contrast to mean field approaches, that usually describes the infinite U limit of the SIAM [5,6,9,10,13–15]. Our results are consistent with those recently obtained by Costi and Zlatić [1] and Yoshida and Oliveira [2], both employing numerical renormalization group theory, and with some recent experimental reports [7,8]. This method is able to capture the low temperature physics, dominated by the Kondo effect as well as the region $T \simeq \Delta$, with Δ the Anderson parameter, where the charge fluctuation processes are dominant.

The thermoelectric figure of merit $Z = S^2 G/\kappa$ [3,5,9,13] is a measure of the usefulness of materials or devices for thermopower generators or cooling systems. Since Z for simple systems varies in inverse proportion to the temperature T, it is convenient to calculate ZT, which indicates the system performance:

$$ZT = \frac{S^2 TG}{\kappa} \tag{1}$$

In ordinary metals, the thermal and electrical conductances are related to the same scattering processes with only weak energy dependence. This is the main reason that metals exhibit lower ZT values. However, in nanoscopic systems the situation changes

* Corresponding author.
E-mail address: rfrancop@unal.edu.co (R. Franco).

http://dx.doi.org/10.1016/j.physe.2014.06.024
1386-9477/

completely, due to the level quantization and the Coulomb interaction, which drastically changes the thermoelectric properties of the system. For ordinary metals, the Wiedemann–Franz law states that the relation between the thermal and electrical conductances, defined by the Lorenz ratio

$$L=\frac{\kappa}{GT} \tag{2}$$

is a constant given by the Lorenz number $L_o=(\pi^2/3)(k_B/e)^2$, where k_B is the Boltzmann constant and e is the electron charge. In our calculations, we worked with the Wiedemann–Franz law in the form

$$W=\frac{L}{L_o}=\frac{3\kappa e^2}{\pi^2 k_B^2 TG}. \tag{3}$$

Employing Eqs. (1) and (3), we can write ZT as

$$ZT=\frac{3S^2e^2}{\pi^2k_B^2W}. \tag{4}$$

This equation shows that the violation of the Wiedemann–Franz law can lead to an increase of ZT in regions where $W<1$. In regions where the Wiedemann–Franz law is valid ($W=1$), only high values of $S>(\sqrt{\pi^2/3})(k_B/e)$ assure $ZT>1$, a necessary condition in order for the system to be employed in thermoelectric devices [3,5,9].

2. Model and theory

We employed the SIAM in the representation of the Hubbard operators to describe an embedded QD, connected to a paramagnetic leads system

$$\begin{aligned}H=&\sum_{\alpha=L,R}\sum_{\mathbf{k},\sigma}E_{\mathbf{k},\alpha}c^{\dagger}_{\mathbf{k},\alpha,\sigma}c_{\mathbf{k},\alpha,\sigma}+\sum_{\sigma}E_{QD,\sigma}X_{QD,\sigma\sigma}\\&+\sum_{\alpha=L,R}\sum_{\mathbf{k},\sigma}\left(V_{\alpha}X^{\dagger}_{QD,0\sigma}c_{\mathbf{k},\alpha,\sigma}+H.c.\right)\\&+(E_{QD,\sigma}+U)X_{QD,dd}\end{aligned} \tag{5}$$

where the first term describes the leads at the right (R) and the left (L) of the QD, and the second corresponds to the QD, considering the presence of a localized QD level with energy $E_{QD,\sigma}$, here $\langle X_{QD,\sigma\sigma}\rangle=n_{QD,\sigma}$, and $\langle X_{QD,\overline{\sigma}\overline{\sigma}}\rangle=n_{QD,-\sigma}$. The third term is the tunneling term, in this the amplitude V_{α} is responsible for the tunneling between the QD and the lead α. For simplicity, we assume symmetric junctions (i.e. $V_L=V_R=V$) and identical leads. The last term is the U Coulomb repulsion between the localized electrons in the QD, taking into account the existence of a level with energy $E_{QD,\sigma}+U$, for the double occupation case, linked to the Hubbard operator $X_{QD,dd}$.

The Hubbard operators are convenient for working with the local state linked to the QD, and are defined in general by $X_{p,ab}=|p,a\rangle\langle p,b|$ [16–19]. The identity relation in the reduced space of the localized states at the QD site, expressed in terms of the Hubbard operators, is

$$X_{00}+X_{\sigma\sigma}+X_{\overline{\sigma}\overline{\sigma}}+X_{dd}=I, \tag{6}$$

where I is the identity operator. Associated with this relation, the occupation numbers for the QD,

$$n_a=\langle X_{aa}\rangle=\left(\frac{-1}{\pi}\right)\int_{-\infty}^{\infty}d\omega\,\mathrm{Im}(G^f_{o\sigma}(z))n_F, \tag{7}$$

satisfy the "completeness" relation

$$n_0+n_{\sigma}+n_{\overline{\sigma}}+n_{dd}=1.0. \tag{8}$$

We use the index $I_x=1,2,3,4$, defined in Table 1, to characterize these X operators.

Representation of the possible transitions present in the finite U atomic SIAM Hamiltonian. $I_x=1,3$ destroy one electron with spin up and $I_x=2,4$ destroy one electron with spin down. We use $\sigma=+$ and $\sigma=-$ instead of $\sigma=\uparrow$ and $\sigma=\downarrow$ to emphasize that the spin belongs to a local electron.

3. The atomic approach for the single impurity Anderson model (SIAM)

In three previous papers [16–18] we developed a simple method that employs the atomic solution of the periodic Anderson model (PAM) as a "seed" to generate approximate Green's functions in order to describe the Kondo physics of the Anderson impurity model. In the paper [18] we develop the theory of the method; we obtain the exact formal Green's functions, valid both for the PAM and for the SIAM, which is given by the Dyson equation

$$\mathbf{G}^f_{\sigma}=\mathbf{M}_{\sigma}\cdot(\mathbf{I}-\mathbf{A}_{\sigma})^{-1}, \tag{9}$$

here $\mathbf{A}_{\sigma}=\mathbf{W}_{\sigma}\cdot\mathbf{M}^{at}_{\sigma}$ and $\mathbf{M}^{at}_{\sigma}$ are the atomic cumulants of the model. From this equation, we can calculate the cumulants $\mathbf{M}_{\sigma}$ as follows:

$$\mathbf{M}_{\sigma}=(\mathbf{I}+\mathbf{G}^f_{\sigma}\cdot\mathbf{W}_{\sigma})^{-1}\cdot\mathbf{G}^f_{\sigma}, \tag{10}$$

and for an impurity located at the origin $\mathbf{W}_{\sigma}$ is given by

$$\mathbf{W}_{\uparrow}(z)=|V|^2\varphi_{\uparrow}(z)\begin{pmatrix}1&1\\1&1\end{pmatrix}, \tag{11}$$

$$\mathbf{W}_{\downarrow}(z)=|V|^2\varphi_{\downarrow}(z)\begin{pmatrix}1&-1\\-1&1\end{pmatrix}, \tag{12}$$

where for a rectangular band with half-width D in the interval $[A,B]$, with $B=A+2D$ we have

$$\varphi_{\sigma}(z)=\frac{1}{2D}\ln\left(\frac{z-B+\mu}{z+A+\mu}\right), \tag{13}$$

where the chemical potential μ appears in $\varphi_{\sigma}(z)$ because $\varepsilon(\mathbf{k},\sigma)=E_{\mathbf{k},\sigma}-\mu$ in $\mathcal{G}^0_{c,\sigma}(\mathbf{k},z)$.

These exact Green's functions can be expressed in terms of the cumulants that are associated with the transitions represented in Table 1

$$\mathbf{G}^f_{\uparrow}(i\omega)=\frac{\mathbf{M}^{\mathbf{at}}_{\mathbf{13}}(i\omega)-|V|^2\varphi_{\uparrow}(i\omega)(m_{11}m_{33}-m_{13}m_{31})\mathbf{I}'}{1-|V|^2\varphi_{\uparrow}(i\omega)(m_{11}+m_{33}+m_{13}+m_{31})}, \tag{14}$$

$$\mathbf{G}^f_{\downarrow}(i\omega)=\frac{\mathbf{M}^{\mathbf{at}}_{\mathbf{24}}(i\omega)-|V|^2\varphi_{\downarrow}(i\omega)(m_{22}m_{44}-m_{24}m_{42})\mathbf{I}}{1-|V|^2\varphi_{\downarrow}(i\omega)(m_{22}+m_{44}+m_{24}+m_{42})}, \tag{15}$$

where

$$\mathbf{I}=\begin{pmatrix}1&1\\1&1\end{pmatrix},\quad \mathbf{I}'=\begin{pmatrix}1&-1\\-1&1\end{pmatrix} \tag{16}$$

and

$$\mathbf{M}^{\mathbf{at}}_{\mathbf{13}}(i\omega)=\begin{pmatrix}m_{11}&m_{13}\\m_{31}&m_{33}\end{pmatrix},\quad \mathbf{M}^{\mathbf{at}}_{\mathbf{24}}(i\omega)=\begin{pmatrix}m_{22}&m_{24}\\m_{42}&m_{44}\end{pmatrix} \tag{17}$$

are the atomic cumulants calculated from the atomic Green's functions. The details of the atomic approach derivation are not given in the present paper, since the cumulants and the atomic Green's function calculations can be found in Ref. [16]. In the same

Table 1

I_x	1	2	3	4
$\alpha=(b,a)$	$(0,+)$	$(0,-)$	$(-,d)$	$(+,d)$

way, we can obtain the conduction $\mathbf{G}_{\sigma}^{cc}(\mathbf{k},\mathbf{k}',i\omega)$ and the cross $\mathbf{G}_{\sigma}^{cf}(\mathbf{k},i\omega)$ Green's functions, whose details of their derivation are included in an electronic archive deposited at the Los Alamos electronic repository [19].

The atomically exact Green's function $G_{\sigma}^{f,at}(z)$ of the atomic problem [16] satisfies a Dyson equation of the same form as Eq. (9), but now in terms of the atomic cumulants

$$\mathbf{G}_{\sigma}^{f,at}=\mathbf{M}_{\sigma}^{at}\cdot(\mathbf{I}-\mathbf{W}_{\sigma}^{\mathbf{o}}M_{\sigma}^{at})^{-1} \tag{18}$$

and from this equation we obtain the exact atomic cumulant $\mathbf{M}_{\sigma}^{at}$

$$\mathbf{M}_{\sigma}^{at}=(\mathbf{I}+\mathbf{G}_{\sigma}^{f,at}\cdot\mathbf{W}_{\sigma}^{o})^{-1}\cdot\mathbf{G}_{\sigma}^{f,at}, \tag{19}$$

where

$$\mathbf{W}_{\uparrow}^{o}(z)=|\Delta|^{2}\varphi_{\uparrow}^{o}(z)\begin{pmatrix}1 & 1\\ 1 & 1\end{pmatrix}, \tag{20}$$

$$\mathbf{W}_{\downarrow}^{o}(z)=|\Delta|^{2}\varphi_{\downarrow}^{o}(z)\begin{pmatrix}1 & -1\\ -1 & 1\end{pmatrix}, \tag{21}$$

and

$$\varphi_{\sigma}^{o}(z)=\frac{-1}{z-\varepsilon_{o}-\mu}. \tag{22}$$

This equation corresponds to the zero-width band located at ε_0, namely the bare conduction Green's function. In the computational calculation we fix the chemical potential at $\mu=0$ and vary the conduction atomic level ε_0 in such a way that the Friedel sum rule can be satisfied [16]

$$\rho_{f\sigma}(\omega)|_{\omega=\mu}=\frac{\sin^{2}(\pi n_{f\sigma})}{\Delta\pi}, \tag{23}$$

where $\rho_{f,\sigma}(\omega)|_{\omega=\mu}$ is the density of states of the localized level at the chemical potential and $n_{f,\sigma}$ is the occupation number per spin of the localized state and $\Delta=\pi V^{2}\rho_{c}(\omega)|_{\omega=\mu}=\pi V^{2}/2D$ is the Anderson parameter.

The approximated atomic cumulant M_{σ}^{ap} (Eq. (19)) is obtained by replacing Eqs. (20)–(22) in Eq. (19) and Green's functions are obtained substituting the cumulants obtained in the same manner described above in Eqs. (14) and (15). This procedure overestimates the contribution of the c electrons [20] because we concentrate them at a single energy level ε_o, and to moderate this effect we replace V^2 with Δ^2 in Eqs. (20)–(21).

4. Thermoelectric properties

Dong and Lei [3] derived the particle current and thermal flux formulas, through an interacting QD connected to leads, within the framework of the Keldysh non-equilibrium Green's functions (GF). The electric and thermoelectric transport coefficients were obtained in the presence of the chemical potential and temperature gradients with the Onsager relation in the linear regime automatically satisfied. We can calculate the linear thermopower

$$S=\left(\frac{-1}{eT}\right)\left(\frac{L_{12}}{L_{11}}\right), \tag{24}$$

the thermal conductance

$$\kappa=\left(\frac{1}{T^{2}}\right)\left(L_{22}-\frac{L_{12}^{2}}{L_{11}}\right), \tag{25}$$

and the electrical conductance

$$G=-\left(\frac{e^{2}}{T}\right)L_{11}; \tag{26}$$

with the transport coefficients given by

$$L_{11}=\frac{2T}{h}\sum_{\sigma}\int\left(\frac{\partial n_{F}}{\partial\omega}\right)\tau_{\sigma}(\omega)\,d\omega, \tag{27}$$

$$L_{12}=\frac{2T^{2}}{h}\sum_{\sigma}\int\left(\frac{\partial n_{F}}{\partial T}\right)\tau_{\sigma}(\omega)\,d\omega, \tag{28}$$

$$L_{22}=\frac{2T^{2}}{h}\sum_{\sigma}\int\left(\frac{\partial n_{F}}{\partial T}\right)\omega\tau_{\sigma}(\omega)\,d\omega, \tag{29}$$

where $n_F(\omega)$ is the Fermi–Dirac distribution function and $\tau_{\sigma}(\omega)=\Gamma^{2}|G_{00,\sigma}(\omega)|^{2}$ is the transmittance for the electrons with spin σ. $G_{00,\sigma}(\omega)$ is the local GF at the QD site, which for a T-shaped lateral QD is

$$G_{00,\sigma}(\omega)=G_{c}^{\sigma}(\omega)+(G_{c}^{\sigma}(\omega))^{2}V^{2}G_{QD}^{\sigma}(\omega), \tag{30}$$

$\Gamma=V^2/\Delta$ with $\Delta=\pi V^{2}\rho_{c}(\omega)|_{\omega=\mu}=\pi V^{2}/2D$ being the mixing width between the QD and the leads, $\rho_c(\omega)=1/2D$ being the DOS for the conduction band, associated with the leads described by a ballistic channel and the GF

$$G_{c}^{\sigma}(\omega)=\frac{-1}{2D}\ln\left(\frac{\omega+D}{\omega-D}\right), \tag{31}$$

where $\omega=\omega+i\eta$ $(\eta\to0^{+})$ and D is the semi-width of the conduction band.

Within the atomic approach the QD GF $G_{\sigma}^{f}(\omega)$ is given by Eqs. (14) and (15).

5. Results and discussion

In our calculations, we chose the following parameters $\Delta=\pi V^{2}\rho_{c}(\omega)|_{\omega=\mu}=\pi V^{2}/2D=1$, with $\mu=0$ being the chemical potential, $D=100\Delta$ the half-width of the conduction band, and $U=20\Delta$ the energy linked to the electronic Coulomb repulsion in the QD; all the energies are expressed in Δ units.

In Fig. 1 we show the electrical conductance G as a function of the QD energy (E_{QD}), for different temperatures. At temperatures $T\simeq\Delta$ the curve exhibits a plateau in the central region, at around the symmetric limit ($E_{QD}=-U/2=-10\Delta$). As we decrease the temperature a destructive interference occurs between the electrons that go through the ballistic channel and the electron that "visits" the quantum dot and returns to the ballistic channel. This is the manifestation of the Kondo effect in that system [1,2,14,16]. As the temperature is decreased, the Kondo effect generates a destructive quantum interference process, associated with the

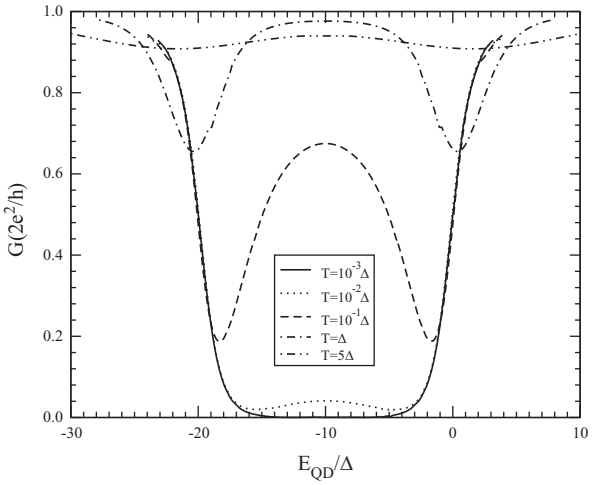

Fig. 1. The electrical conductance G vs. E_{QD} for several temperatures.

Fano anti-resonant character of the system, which causes the depression of the electrical and thermal transport properties at around the symmetric point of the model $E_{QD} = -U/2 = -10\Delta$.

For intermediate temperatures, there are two dips at around the regions where strong charge fluctuations in the QD exist, linked to the entrance of one electron in the QD (right dip) and two electrons in the QD (left dip). The plateau in G between those two dips is associated with the competition between the cotunneling process, including the Kondo effect, which has the characteristic of being mediated by virtual quantum processes, and the sequential resonant tunneling associated with the difference of energy required to put a second electron in the QD (U parameter – Coulomb blockade) [21–23]. When the temperature increases over the Kondo temperature, the Kondo effect disappears, and with it the cotunneling process linked to the spin-flip process. The resonant tunneling and the Coulomb blockade are responsible for the minimum dips in G. The non-unitary value between the dips is due to the cotunneling process, not suppressed with the increase of the temperature. These results are in agreement with recent reports obtained by NRG [2] in the same system studied by us [13], and in a qualitatively similar system of diluted magnetic impurities introduced into a conduction channel [1].

Fig. 2 shows the results of the thermal conductivity normalized by the temperature, $3e^2\kappa/T\pi^2k_B^2$ vs. the QD energy E_{QD} at different temperatures. At very low temperatures, the behavior is similar to that obtained for the electrical conductance G vs. E_{QD} (see Fig. 2), but at $T = 10^{-2}\Delta$ it is evident that in the Kondo regime $3e^2\kappa/T\pi^2k_B^2 \neq G$ (see Fig. 2). Because of the Fermi liquid character of the system we expected complete equality, associated with the validity of Wiedemann–Franz law; that is, the system loses its Fermi liquid character at low temperatures in the Kondo regime, and as a consequence the Wiedemann Franz law is no longer valid. This is a very reasonable result, taking into account the strongly correlated character of the system in the Kondo regime at low temperatures. The destructive quantum interference processes linked to this configuration, cause a minimum in the Kondo regime at low temperatures. At intermediate temperatures, the minima in it are associated with the charge fluctuations in the QD, at the energy values required for the entrance of one electron ($E_{QD} \sim \mu = 0.0\Delta$) and two electrons ($E_{QD} \sim \mu + U = 20\Delta$) in the QD. Our results are very similar to those reported by Yoshida and Oliveira [2] in the same system studied by us, and to the results of Costi and Zlatić in a system of diluted magnetic impurities introduced into a conduction channel [1], employing NRG treatment in both cases.

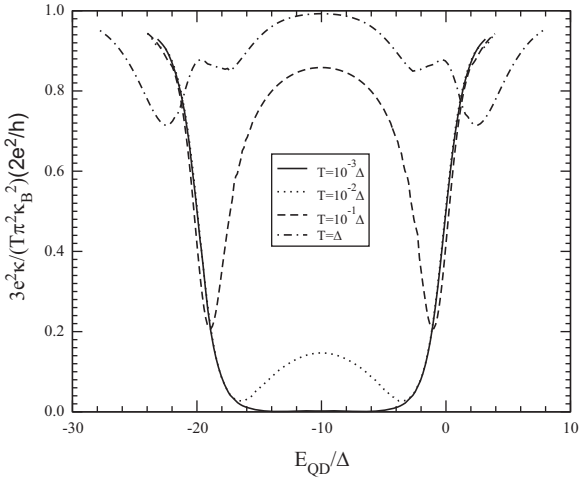

Fig. 2. The quantity $3e^2\kappa/T\pi^2k_B^2$ vs. E_{QD} for different temperatures.

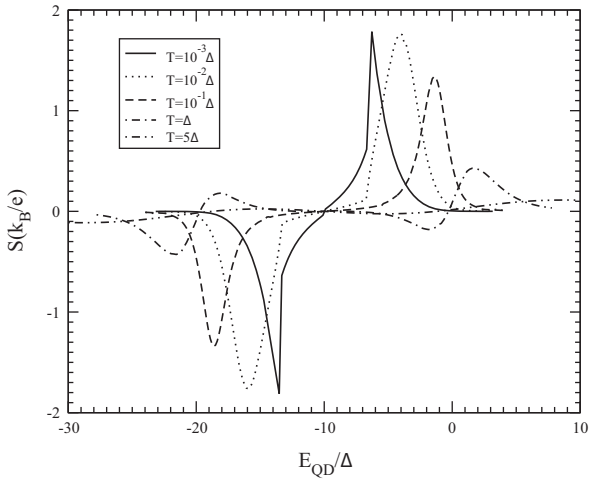

Fig. 3. Linear thermopower (S) vs. the QD energy (E_{QD}) for different temperatures.

In Fig. 3 we show the linear thermopower (S) vs. the gate voltage of the QD, here represented by the QD energy (E_{QD}), at different temperatures. The linear thermopower result shows the oscillatory behavior characteristic of the system, similar to that reported for the immersed QD case [1–5,9,13], but changing the sign of S at low temperatures; the change of this sign was previously reported by Yoshida and Oliveira [2] employing NRG and Castellanos et al. [14] using the X-Boson approach for the single impurity Anderson model in the same system, and by Costi and Zlatić in a system of diluted magnetic impurities [1].

As in the embedded QD case [1–5,9,13], the oscillatory behavior of S is linked to the different regimens of the system and the derivative of the density of states for the QD, as a function of the energy [3,13]. The T-shaped QD exhibits an important difference when compared to the immersed case: the higher S values are obtained when we lower the temperatures, which agrees with previous results obtained for the same system (T-shaped QD) employing NRG by Yoshida and Oliveira [2]. Qualitatively, the behavior of S is similar to that reported for the immersed QD case, at low temperatures the S sign changes at around the symmetric limit ($E_{QD} = -U/2 = -10\Delta$), where due to the Kondo resonance in the density of states the system exhibits a symmetry electron–hole. Since the contribution of electrons is minus the contribution of holes, S is zero in the symmetric limit point. The change in S is shown in the Kondo region ($-3U/4 < E_{QD} < -U/4$), associated with different contributions of holes and electrons at the sides of the symmetric limit point. At higher temperatures, the peaks in S are displaced to the regions of strong charge fluctuations, at $E_{QD} \sim \mu = 0.0\Delta$, where the charge fluctuations are associated with single occupation of the QD, and at $E_{QD} \sim \mu + U = 20\Delta$, where the charge fluctuations are associated with the double occupation of the QD.

Fig. 5 shows the ZT vs. the QD energy E_{QD} for different temperatures. At high temperatures, the system has poor thermal efficiency in all the regimes, but at lower temperatures in the regions where the thermopower exhibits its maximum value, ZT is close to the unit ($ZT \sim 0.8$). This behavior is the opposite of that obtained for the QD immersed case, where the ZT value grows with the increase of the temperature [1,13] in the transition between the empty QD and the Kondo regimes. Since ZT is proportional to the S^2 (cf. Eq. (4)), the maximum value obtained for this quantity closely follows the behavior of the thermopower, as indicated in Fig. 3. On the other hand, the Wiedemann–Franz law (WFL) $W = 3e^2\kappa/\pi^2k_B^2TG$, represented in Fig. 4 as a function of the QD energy E_{QD}, shows that at low temperature, due to its high

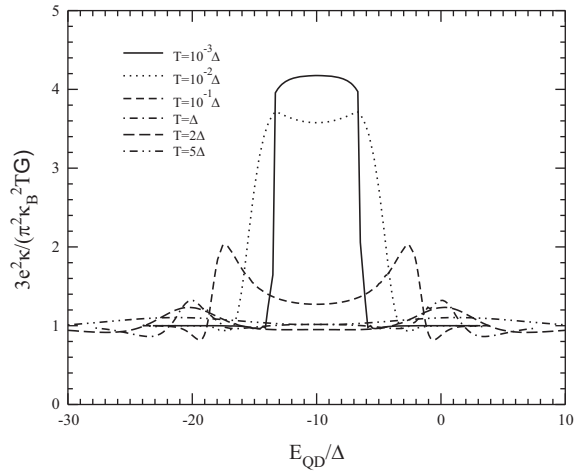

Fig. 4. The Wiedemann–Franz law $W = 3e^2\kappa/TG\pi^2k_B^2$ vs. E_{QD} for different temperatures.

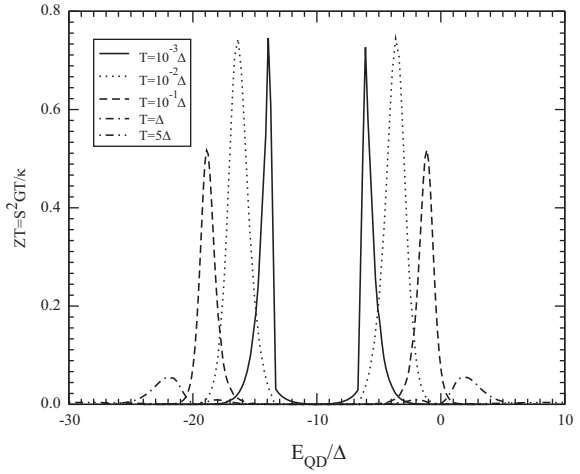

Fig. 5. The product of the thermal figure of merit and the temperature ZT vs. E_{QD} for different temperatures.

value, it contributes to decreasing the ZT value in the Kondo region at around the symmetric limit.

Recently, the violation of the WFL due to the existence of a Fano antiresonance, linked to the presence of at least two conduction channels, a resonant one and a non resonant one, was linked to the enhancement of the product ZT in a double quantum dot molecule, without electronic correlation in the dots [24]; a result in agreement with other recent papers that associate the violation of the WFL with the enhancement of the ZT value [25,26]. The system considered in this paper, we have the Fano anti-resonant character, associated with the existence of a resonant channel (the QD) and a direct non-resonant channel (the quantum wire), where Fano antiresonance is manifest in the minimum-dips for the electrical conductance G, when charge fluctuations in the QD are present. Our results show the violation of the WFL in the Kondo regime at low temperatures, with the highest ZT values obtained at the "limits" of the Kondo regime at low temperatures, near the beginning of the charge fluctuations region in the QD, where a strong Fano anti-resonant character is present. That is, our results are in qualitative agreement with those obtained by Gómez-Silva et al. An important difference with respect to the Gómez-Silva et al. paper is that in our case we have strong electronic correlation in the QD, and the WFL violation is not due to the Fano character of the system. In our case, the many-body interactions at the QD in

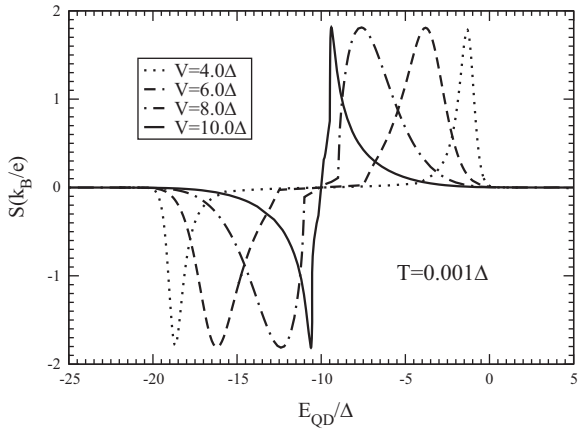

Fig. 6. Linear thermopower (S) vs. the QD energy (E_{QD}) for different hybridizations.

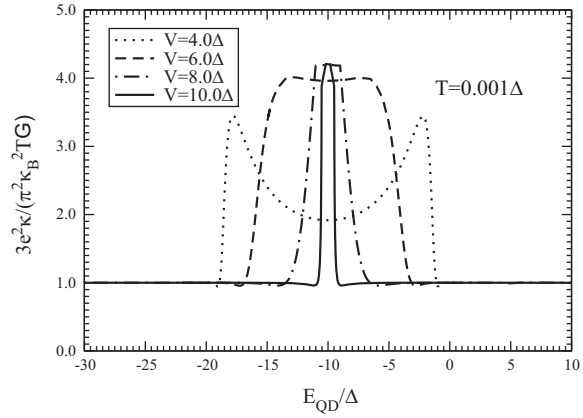

Fig. 7. The Wiedemann–Franz law $W = 3e^2\kappa/TG\pi^2k_B^2$ vs. E_{QD} for different hybridizations.

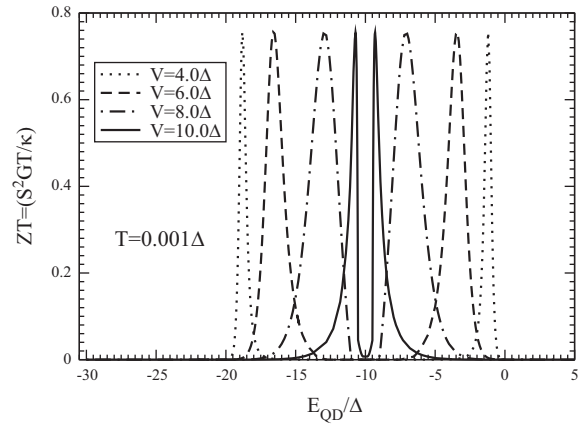

Fig. 8. The product between the thermal figure of merit and the temperature ZT vs. E_{QD} for different hybridizations.

the Kondo regime at low temperatures are the cause of this condition.

In Fig. 6, we show the linear thermopower (S) vs. the gate voltage of the QD, here represented by the QD energy (E_{QD}), at different hybridizations. The main effect of the increase of the hybridization is to diminish the distance between the S peaks. This effect seems to be related to the violation of the Wiedemann–Franz relation, as indicated in Fig. 7, because according to this

figure the region where W is violated diminishes with the increase of the hybridization. These two effects produce the ZT curves indicated in Fig. 8. The ZT maximum is completely related to the maximum of the thermopower once ZT is proportional to S^2, whereas the Wiedemann–Franz violation only contributes to diminishing the ZT values in the region between the peaks, once ZT is inversely proportional to W and its value in that region is greater than unity (see Eq. (4)).

6. Conclusions

We studied thermoelectric transport properties through a QD side coupled to a ballistic conduction channel. The results obtained are consistent with some earlier papers employing NRG [1,2]. In this way, we conclude that the U finite atomic approach for the SIAM is an adequate theoretical tool for computing the thermoelectric transport properties of the model, with the advantage of its simplicity and the analytical derivation of the GF's [16].

The results for the product of the thermoelectric figure of merit and the temperature ZT show two maximum values, at low temperatures, which are completely determined by the interplay between the thermopower behavior and the violation of the Wiedemann–Franz relation close to the "limits" of the Kondo regime. Under these conditions, the charge fluctuations are not present (the occupation in the QD $n_{QD} \simeq 1$), but strong spin fluctuations are expected, linked to the Kondo effect. That situation would present the best possibility of practical application of the system in the development of thermoelectric devices.

Our results are in qualitative agreement with a recent paper that links an enhancement of the thermal efficiency ZT with the existence of a Fano anti-resonant character that causes the violation of the WFL [24], and with other papers that associate the ZT improvement with the violation of the WFL [25,26]. The values of the thermal efficiency ZT show an enhancement in a region of a set of parameters where a violation of the WFL is present, with a Fano anti-resonant character, but the cause of the violation of the WFL is not linked to the Fano anti-resonant character, it is due to many-body interactions in the QD. We conclude that a system with a Fano anti-resonant character and simultaneously a violation of the WFL would exhibit an enhancement of the thermal efficiency ZT, without the violation of the WFL necessarily being due to the Fano character of the system.

Finally, our results for the thermopower S and electrical conductance G are qualitatively very similar to those reported experimentally for a QD immersed in a conduction channel [7,8]; taking into account that, for the T-shaped QD case, are present dips and not tips in G vs. E_{QD}, and the thermopower sign of S vs. E_{QD} changes ($S \rightarrow -S$) [1,2,15], this, because to the destructive quantum interference process associated to the quantum scattering of electrons and holes by the QD; that in the immersed QD case is manifested by a constructive quantum interference process.

Acknowledgments

We thank the financial support of DINAIN and DIB (Colombia National University), COLCIENCIAS (Colombia) and the Brazilian National Research Council CNPq. R. Franco and J. Silva-Valencia thank the support of the International Centre for Theoretical Physics (ICTP)-Trieste, where part of this work was done.

References

[1] T.A. Costi, V. Zlatić, Phys. Rev. B 81 (2010) 235127.
[2] M. Yoshida, L.N. Oliveira, Physica B 404 (2009) 3312.
[3] B. Dong, X.L. Lei, J. Phys. Condens. Matter 14 (2002) 11747.
[4] D. Boese, R. Fazzio, Europhys. Lett. 4 (2001) 576.
[5] M. Krawiec, K.I. Wysokiński, Phys. Rev. B 73 (2006) 075307.
[6] M. Krawiec, K.I. Wysokiński, Phys. Rev. B 75 (2007) 155330.
[7] R. Scheibner, H. Buhmann, D. Reuter, M.N. Kiselev, L.W. Molemkamnp, Phys. Rev. Lett. 95 (2005) 176602.
[8] R. Scheibner, E.G. Novik, T. Borzenko, M. König, D. Reuter, A.D. Wieck, H. Buhmann, L.W. Molenkamp, Phys. Rev. B 75 (2007) 041301.
[9] R. Sakano, N. Kawakami, J. Mag. Mag. Mater. 310 (2007) 1136.
[10] R. Sakano, T. Kita, N. Kawakami, J. Phys. Soc. Jpn. 76 (2007) 074709.
[11] C.W. Chang, D. Okawa, A. Mujumdar, A. Zettl, Science 314 (2006) 1121.
[12] Olli-Pentti Saira, M. Meschke, F. Giazotto, A.M. Savin, M. Möttonen, J.P. Pekola, Phys. Rev. Lett. 99 (2007) 027203.
[13] R. Franco, J. Silva-Valencia, M.S. Figueira, J. Mag. Mag. Mater. 320 (2008) 242.
[14] R. Castellanos, R. Franco, J. Silva-Valencia, M.S. Figueira, Physica A 389 (2010) 5814.
[15] R. Franco, J. Silva-Valencia, M.S. Figueira, J. Appl. Phys. 103 (2008) 07B726.
[16] T. Lobo, M.S. Figueira, M.E. Foglio, Nanotechnology 21 (2010) 274007.
[17] T. Lobo, M.S. Figueira, M.E. Foglio, Nanotechnology 17 (2006) 6016.
[18] M.E. Foglio, T. Lobo, M.S. Figueira, AIP Adv. 21 (2012) 032139.
[19] M.E. Foglio, T. Lobo, M.S. Figueira, Green's functions for the Anderson model: the atomic approximation, 2010 arXiv:0903.0139[cond-mat].
[20] B.R. Alascio, R. Allub, A.J. Aligia, Phys. C: Solid State Phys. 13 (1980) 2869; B.R. Alascio, H. Wio, A. Lopez, Z. Phys. B Cond. Mat. 36 (1979) 37.
[21] S. De Franceschi, S. Sasaki, J.M. Elzerman, W.G. van der Wiel, S. Torucha, L. P. Kowenhoven, Phys. Rev. Lett. 86 (2001) 878.
[22] S. Andergassen, V. Meden, H. Schoeller, J. Splettstoesser, M.R. Wegewijs, Nanotechnology 21 (2010) 272001.
[23] R.A. Osorio, J. Bjornholm, J.-M. Lehn, M. Ruben, H.S.J. van der Zant, J. Phys. Condens. Matter 20 (2008) 374121.
[24] G. Gómez-Silva, O. Ávalos-Ovando, M.L. Ladrón de Guevara, P.A. Orellana, J. Appl. Phys. 111 (2012) 053704.
[25] Piotr Trocha, Jozef Barnas, Phys. Rev. B 85 (2012) 085408.
[26] Bjorn Kubala, Jurgen Konig, Jukka Pekola, Phys. Rev. Lett. 100 (2008) 066801.